

See discussions, stats, and author profiles for this publication at: <https://www.researchgate.net/publication/360180569>

# Surface Roughness Effects on Ionic Polymer–Metal Composite (IPMC) Sensitivity for Compression Loads

Conference Paper · April 2022

---

CITATIONS  
0

READS  
53

5 authors, including:



William S Nagel  
University of Utah  
14 PUBLICATIONS 51 CITATIONS

[SEE PROFILE](#)



Matteo Aureli  
University of Nevada, Reno  
57 PUBLICATIONS 1,399 CITATIONS

[SEE PROFILE](#)



Kam K Leang  
University of Utah  
162 PUBLICATIONS 4,486 CITATIONS

[SEE PROFILE](#)

Some of the authors of this publication are also working on these related projects:



Study of Taylor-Couette-Poiseuille Flow at Submerged Cryogenic Induction Motor Air Gap [View project](#)



High Speed Atomic Force Microscopy [View project](#)

# Surface Roughness Effects on Ionic Polymer-Metal Composite (IPMC) Sensitivity for Compression Loads

William S. Nagel<sup>1</sup>, Omar A. Hussain<sup>1</sup>, Omid Fakharian<sup>2</sup>, Matteo Aureli<sup>2,\*</sup>,  
and Kam K. Leang<sup>1,\*</sup>

<sup>1</sup>Design, Automation, Robotics, & Control (DARC) Lab, Robotics Center, Department of Mechanical Engineering, University of Utah, Salt Lake City, Utah, 84112, USA

<sup>2</sup>Department of Mechanical Engineering, University of Nevada, Reno, Reno, NV 89557, USA

## ABSTRACT

The soft and compliant nature of ionic polymer-metal composite (IPMC) sensors has recently been investigated for various applications in soft robotic and mechatronic devices. Recent results of physics-based chemoelectromechanical modeling suggest that IPMC asymmetric surface roughening may enhance the sensitivity under compression. This paper presents initial experimental results on IPMC compression sensors fabricated with varying degrees of asymmetric surface roughness. The roughness is created through a simple mechanical sanding process on the base polymer material, referred to as “polymer abrading technique”, followed by traditional electroless plating to create electrodes. Sample sensors are characterized by measuring the voltage response under different compressive loads. The results show consistently increased sensor sensitivity of the asymmetrically roughened IPMCs versus a control sample. Sensitivity increases non-monotonically with rougher electrode surfaces, where maximum sensitivity of about 0.0433 mV/kPa is achieved with sensor electrodes with 53–74  $\mu\text{m}$  abrasions. More variability is also observed through augmented electrode roughness, suggesting greater flexibility for IPMC sensor design. These results align with predictions from the existing physics-based chemoelectromechanical model.

**Keywords:** Ionic polymer-metal composite sensor, electroactive polymer, compression strain sensing, polymer abrading technique

## 1. INTRODUCTION

Ionic polymer-metal composites (IPMCs) are electroactive polymers that are soft and compliant in nature, which has led to their use in various soft robotic and mechatronic systems and devices.<sup>1,2</sup> The chemoelectromechanical behavior of IPMCs, relating deformation and charge flow through the material, allows for them to be used as low-power actuators<sup>3–5</sup> or self-powered sensors. Some examples of applications of IMPC sensing modalities include flow sensing cilia structures,<sup>6</sup> compliant surgical instruments,<sup>7</sup> and pose-measuring smart gloves.<sup>8</sup>

While the sensing application for IPMCs is well researched, devices typically configure the material to undergo bending deformations.<sup>9–11</sup> Experiments have demonstrated that IPMCs are capable of measuring compression strain deformations,<sup>12–14</sup> although this modality suffers from very low sensitivity between mechanical deformation and the material’s electrical response. A theoretical explanation of the sensing behavior of IPMCs under compression was first offered in 2017.<sup>15</sup> Building on these findings, our group has recently developed a minimal chemoelectromechanical model that relates applied mechanical pressure to the voltage and current observed in the material.<sup>16</sup> Specifically, this model shows that asymmetry of the mechanical properties in the electrode polymer-metal interfaces is directly related to the sensitivity of the material under pressure loading. It is also demonstrated that advanced manufacturing techniques can be leveraged to improve pressure sensitivity for these “engineered IPMCs” (eIPMCs) by additively introducing micro- or macro-scale features, for example with inkjet printing and fused deposition modeling 3D-printing, onto what becomes one of the electrodes of the sensor before plating the material.

---

\*Corresponding authors’ emails: maureli@unr.edu (M. Aureli) and kam.k.leang@utah.edu (K. K. Leang)

While compression sensing in eIPMCs has been successfully demonstrated, fabrication of these engineered sensors requires fairly specialized equipment and techniques that might not be readily available to IPMC researchers. In this work, for the first time, we propose IPMC compression sensors with asymmetric electrodes by design realized via a simple, fast, and cost-effective technique based on differential abrasion of the ionic polymer surfaces before conventional plating. Samples fabricated with this technique are tested in compression under open-circuit voltage measurement conditions. Results demonstrate the effectiveness of this fabrication method against conventional IPMC sensors.

The scientific contributions of this work are (1) the presentation of a hardware-less fabrication technique in which eIPMC electrode-metal interface asymmetry is directly augmented during polymer preparation, and (2) the characterization of five eIPMC sensor variants as compression sensors, where the effects of surface roughness are experimentally compared to the sensors' sensitivity and variability. It is also expected that this technique will help IPMC researchers start experimenting with the concept of eIPMCs and eIPMC-based compression sensors.

## 2. MODEL OF IPMC COMPRESSION-SENSING BEHAVIOR

The sensing behavior of IPMCs under compression has only recently been analytically described,<sup>15</sup> and thus modeling this behavior remains an active area of research. Our group has previously determined a minimal linearized chemoelectromechanical model for the eIPMC concept depicted in Fig. 1, describing the sensing behaviors of IPMCs with engineered metal-polymer interfaces, in this case localized at the ground electrode.<sup>16</sup>

A minimal one-dimensional mechanical model describing the dilatation  $\Delta$  (or local relative change in volume) of an eIPMC based on the engineered feature sizes can be chosen as

$$\Delta(x, t) = -\frac{p(t)/E_p}{1 + \alpha \exp[-(x/d_f)^2]}, \quad (1)$$

where  $p(t)$  is the applied pressure on the eIPMC,  $E_p$  is the Young's modulus of the polymer,  $x$  is the direction of compression,  $d_f$  is the engineered polymer feature height, and  $\alpha$  is a tuning parameter representing the measure of the electrode polymer-metal asymmetry included in the absence of a more detailed micromechanical homogenization. In particular,  $\alpha = 0$  represents when the electrodes are nominally flat. In our previous work,<sup>16</sup> a physical interpretation of the parameter  $\alpha$  has been proposed in terms of polymer and metal Young's moduli and polymer vs. metal volume fraction at the interface.

Linearized one-dimensional versions of Poisson's equation, governing the relationships between electric potential  $\psi$  and free charge in the eIPMC, and the generalized Nernst-Planck equation, establishing the conservation of charge in the eIPMC, describe the eIPMC chemoelectromechanical behavior as<sup>17</sup>

$$-\varepsilon \frac{\partial^2 \psi(x, t)}{\partial x^2} = F\{c(x, t) - c_0[1 - \Delta(x, t)]\}, \quad (2)$$

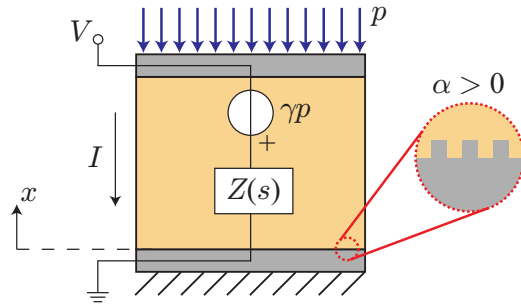


Figure 1. Schematic of eIPMC compression sensor as lumped parameter circuit. Idealized metal-polymer features of the engineered electrode are highlighted.

$$\frac{\partial c(x, t)}{\partial t} + c_0 \frac{\partial \Delta(x, t)}{\partial t} = D \left[ \frac{\partial^2 c(x, t)}{\partial x^2} + \frac{Fc_0}{RT} \frac{\partial^2 \psi(x, t)}{\partial x^2} \right]. \quad (3)$$

Here, parameter  $\varepsilon$  is the eIPMC dielectric constant (assumed uniform in the material domain),  $F$  is Faraday's constant,  $c(x, t)$  is the concentration of mobile counterions,  $c_0$  is the concentration of fixed ions,  $D$  is the counterion diffusivity in the bulk polymer,  $R$  is the universal gas constant, and  $T$  is the eIPMC temperature. These coupled equations can be solved through matched asymptotic expansions, to obtain linear time-invariant (LTI) relationships which describe the eIPMC behavior as a sensor (details are omitted for brevity but can be found in our previous work<sup>16</sup>). A direct computational model can also be used to solve the coupled equations governing the IPMC behavior.

In the Laplace domain, the eIPMC sensor behavior can be characterized via the following expression, involving current output  $I$  (per nominal surface area), external pressure  $P$  inducing mechanical deformation, and voltage response  $V$  at the eIPMC electrodes

$$I(s) = \frac{s}{2(s+1)} V(s) + \frac{s\gamma}{2(s+1)} P(s) = Y(s)V(s) + G(s)P(s), \quad (4)$$

where  $s$  is the Laplace variable,  $\gamma = \alpha/(1+\alpha)$  is a representation of the mechanical asymmetry present in the eIPMC, and  $Z(s) = 1/Y(s)$  describes the LTI impedance of the lumped parameter model of the sensor.

This work is focused on evaluating the open-circuit voltage as the eIPMC sensor output under compression, thus  $I(s) = 0$ . With this assumption, the relationship between applied pressure and sensor open-circuit voltage  $V_{OC}$  is further simplified to

$$V_{OC}(s) = -\frac{G(s)}{Y(s)} P(s) = -\gamma P(s). \quad (5)$$

Therefore, the chemoelectromechanical model for eIPMC sensors shows that the open-circuit voltage response will instantaneously change with changes in pressure. Most importantly, the mechanical asymmetry in the eIPMC electrode is proportional to the sensor sensitivity. Thus, more mechanical asymmetry through parameter  $\gamma$  will increase the magnitude of the sensor response.

### 3. ENGINEERED IPMC MANUFACTURING

Based on the chemoelectromechanical model of eIPMCs as compression sensors, methods for manufacturing eIPMCs with mechanical asymmetries in the polymer-electrode interfacial topography are necessary. Our group's previous work has demonstrated successful fabrication approaches with inkjet-printing, filament-based fused-deposition manufacturing (3D printing), and stencil printing of eIPMCs or their features.<sup>16</sup> This work instead chooses to leverage conventional IPMC manufacturing to introduce asymmetric electrode-polymer features during the Nafion polymer sheet preparation step. Specifically, an abrasive surface is used to roughen the surface of one side of the Nafion polymer sheet to serve as the engineered electrode of the eIPMC; hence this method is denoted the "polymer abrading technique".

Shown in Fig. 2, the polymer abrading technique for fabricating eIPMCs consists of (a) removing small amounts of the ionomer material via sanding with a roughened surface (e.g., sandpaper), (b) cleaning through soakings in acid and de-ionized water then electroless plating of the electrodes, and (c) cutting the material to size for the desired application. In this work, sample swatches are extracted for experimental validation, although general 2D shapes can be obtained through this method as desired.

First, one side of the Nafion membrane sheet is sanded unidirectionally with an abrasive surface to introduce the geometric asymmetry in the electrode interface region of the IPMC's engineered electrode. By roughening one side of the Nafion, the engineered features in the eventual metal-polymer interface are naturally introduced to the membrane rather than through additive manufacturing procedures such as 3D-printing the features onto a membrane sample. The size of these features is approximately controlled through the roughness of the abrasive material, or sandpaper grit rating.<sup>18</sup> It is noted, however, that the grit only gauges the average particle size of the abrasive material and does not guarantee interface feature sizes.

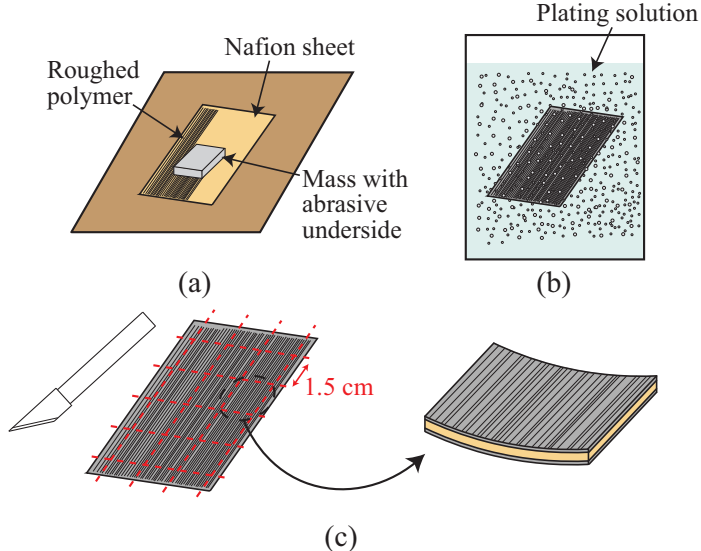


Figure 2. Asymmetric metal-polymer manufacturing technique for engineered IPMCs: (a) A sheet of ionomer polymer material, such as Nafion, is abraded on one side. Here a mass with sandpaper moves along the surface in a uniform direction for the entire polymer sheet. (b) The polymer sample is prepared and cleaned in soaking procedures with de-ionized water and acid solutions, then plated through an impregnation reduction chemical process. (c) The plated sample is cut to size for application, in this work square swatches of 1.5 cm  $\times$  1.5 cm size.

Impurities in the Nafion membrane are removed through pre-treatment cleaning. The sample is chemically cleaned with 3% hydrogen peroxide ( $H_2O_2$ ) followed by a subsequent rinse in 1 M sulfuric acid ( $H_2SO_4$ ), both at 65°C for 45 minutes each with a transition soaking in de-ionized water (DI water) at room temperature for 15 minutes. After rinsing in  $H_2SO_4$  the sample is soaked for 45 minutes in 65°C DI water to conclude the cleaning cycle. This process is conducted twice to adequately clean the Nafion for plating.

After cleaning, the Nafion sample is plated through an electroless chemical procedure. The cleaned Nafion is lightly stirred in a 0.02 M platinum solution at room temperature for approximately four hours. Then, to metalize platinum particles in the surface layers of the membrane, the sample is reduced in a sodium borohydride ( $NaBH_4$ ) solution for three hours, gradually heating up to 65°C. Afterward, the treated sample is cleaned in 0.5 M  $H_2SO_4$  and DI water for 45 minutes and 1.5 hours, respectively. This primary plating procedure is repeated three times to ensure enough platinum is deposited to enhance surface conductivity. A secondary plating procedure is then performed on the sample, where the membrane is soaked in an aqueous tetraamineplatinum (II) chlорidemonohydrate ( $[Pt(NH_3)_4] \cdot Cl_2H_2$ ) solution for three hours, then washed with sulfuric acid and DI water. Again this process is repeated about three times to further ingress of platinum into the membrane. Finally, the platinum-plated sample is soaked in a 1 M lithium chloride ( $LiCl$ ) solution for 24 hours.

The manufactured eIPMC sample sheet is now ready to be cut to size for the application of interest. This work is interested in quantifying the sensitivity of eIPMCs using the abrading Nafion technique for different surface roughnesses. Therefore five swatches (1.5 cm  $\times$  1.5 cm) are cut from the eIPMC sheet, as shown in Fig. 3(a). It is noted that more general 2D shapes can be obtained during this final step depending on the particular application.

#### 4. EXPERIMENTAL INVESTIGATION AND DISCUSSION

The performance under compression of eIPMC sensors fabricated through the polymer abrading technique is investigated next. Five eIPMC sample sheets are manufactured using the procedure outlined in the previous section: four sheets are produced using the sandpaper grits cataloged in Table 1; the average size of the abrading particles for the grit ratings are also listed here. A fifth sheet does not include the abrading step and is denoted “control sample”. It is noted that the theoretical sensitivity of an eIPMC sensor with no sanding operation would be 0 mV/kPa due to symmetric electrode interfaces between the two electrodes ( $\alpha = 0, \gamma = 0$ ), but imperfections

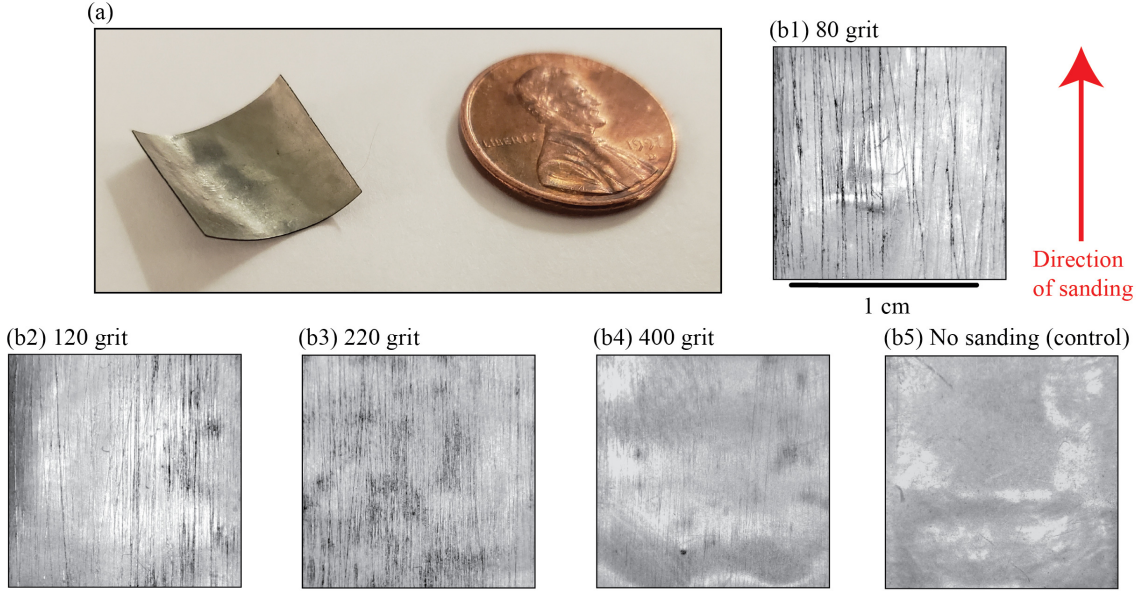


Figure 3. (a) Asymmetric metal-polymer eIPMC sample manufactured using the polymer abrading technique. (b) Surface profiles of the engineered electrode using various sandpaper grit ratings.

in the Nafion membrane and the resulting electrode growth will result in some small voltage response from the control samples in practice.<sup>15</sup> Five sample swatches are cut from each of the activated eIPMC sheets. The sanded surfaces of one of these swatches for each sample type are shown in Fig. 3(b). It can be seen in these images that roughening the Nafion membrane surface results in visible electrode features even after multiple plating cycles. This observation suggests that asymmetrically rough interfaces are generally preserved after plating.

The compression experiment setup is shown in Fig. 4(a). A hydrated eIPMC sample swatch is inserted into the loading mechanism. Pressure is applied to the lever-arm mechanism which in turn compresses the sample onto a fixed load cell. Because both the eIPMC open-loop voltage and load cell signal are very small (millivolts), conditioning circuits are also designed to amplify the signals to be read by a data acquisition system (National Instruments PCI-6221); this circuit schematic is shown in Fig. 4(b). A non-inverting amplifier with a 10 V/V gain increases the eIPMC voltage  $V_{eIPMC}$ , while an instrumentation amplifier circuit structure amplifies the differential voltage of the load cell  $V_{LC}$ . Reported eIPMC voltage values correct for this amplification ratio after acquisition and the load cell is calibrated with known sample weights to determine the pressure applied to the eIPMC sensor.

Voltage responses are measured for each eIPMC sample swatch over three trials each. One loading trial consists of applying various pressure magnitudes to the eIPMC sensor, ranging between about 10–200 kPa over short loading times. The pressures are applied by hand over a trial time of 60–100 seconds so the sample remains sufficiently hydrated. An example of the voltage responses of the eIPMC and load cell is shown in Fig. 5(a). For each spike in the load cell signal, an average pressure is calculated over the compression interval. The

Table 1. Effective size of abrasives corresponding to grit ratings used in sample preparation.<sup>18</sup>

Sandpaper grit	Abrading material particle size ( $\mu\text{m}$ )
80 grit	170 – 210
120 grit	105 – 125
220 grit	53 – 74
400 grit	20.6 – 23.6

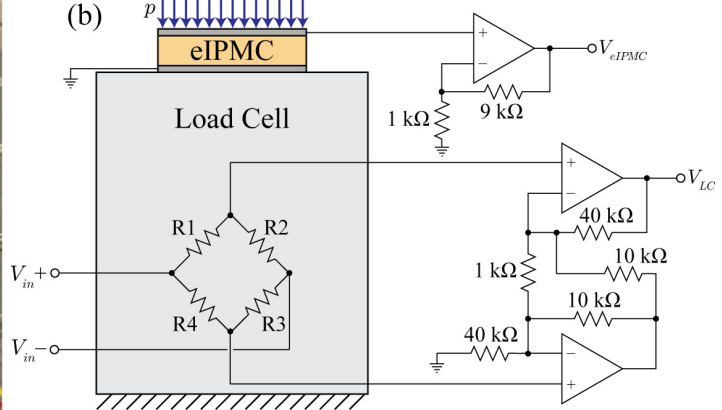
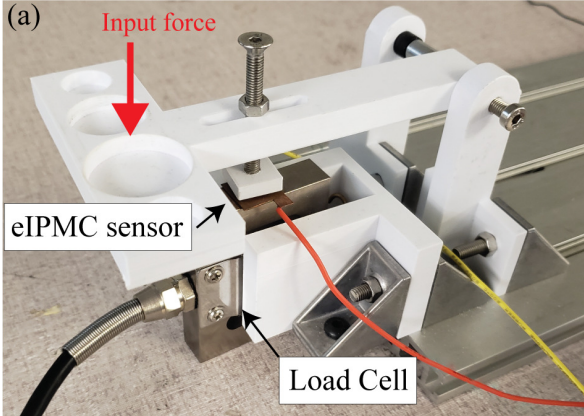


Figure 4. (a) Compression experiment setup. (b) Circuit diagram of the eIPMC and load cell conditioning circuits. The eIPMC voltage is increased using an amplifying circuit with a gain of 10 V/V, and load cell potential is conditioned using an instrumentation amplifier configuration.

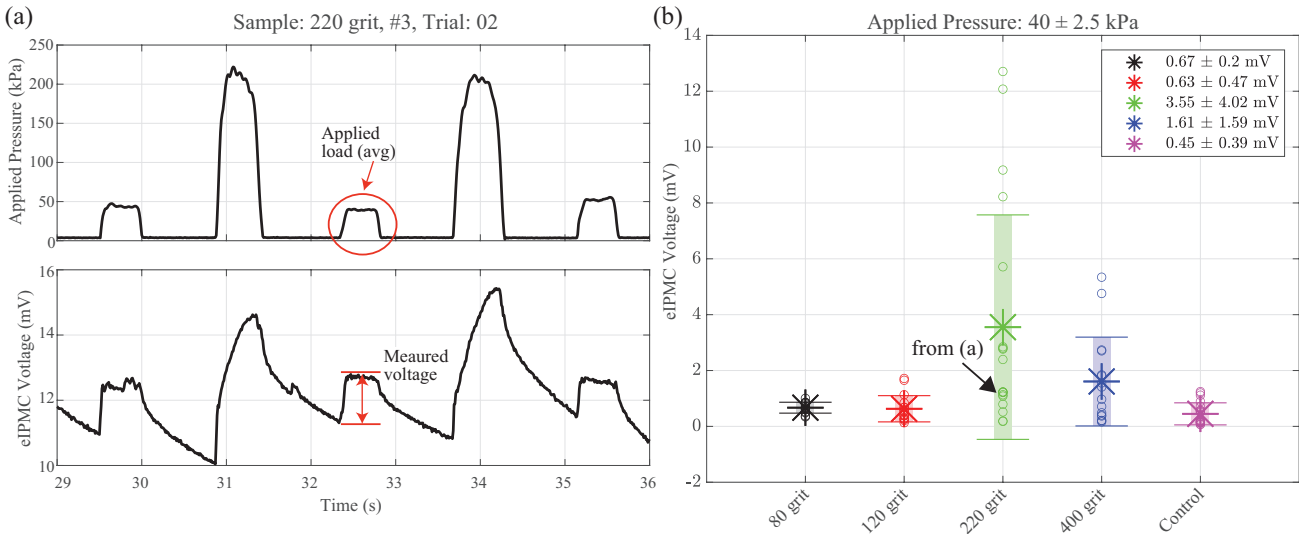


Figure 5. (a) Excerpt of a representative eIPMC time response in compression experiment: applied pressure (top) and eIPMC output voltage (bottom). Average pressure and change in voltage are calculated and treated as a single loading cycle as indicated. (b) Voltage responses of eIPMC compression sensors for pressures of magnitude 40 kPa ( $\pm 2.5$  kPa). Average values and standard deviations are reported for each eIPMC sensor variant.

eIPMC voltage response is calculated over this interval to be the change in voltage from the start of the applied pressure to the maximum measured voltage over the interval. It can be seen that the eIPMC sensor response is proportional to the magnitude of the applied pressure, a behavior that is predicted from the compression model for eIPMCs open-circuit voltage.<sup>16</sup> There is an additional drift in the measured response, a nonlinear effect likely due to dehydration and natural geometric bending of the eIPMC samples over time.

Next, the eIPMC sensor responses to all applied pressures are found over all trials and compared between sensor abrasion levels. The sensor responses for one pressure magnitude are shown in Fig. 5(b); this plot is for all 40 kPa loads within  $\pm 2.5$  kPa. It is observed that the control sensor has the lowest average response at 0.45 mV, which is consistent with what the eIPMC compression model predicts. The 220 grit samples exhibit the largest average response at 3.55 mV, an almost eightfold increase in sensitivity over the control sensor. Although more responsive on average, the 220 grit samples also demonstrate a larger variance in response magnitudes with a standard deviation of 4.02 mV, a tenfold increase over the control sensors' standard deviation of 0.39 mV.

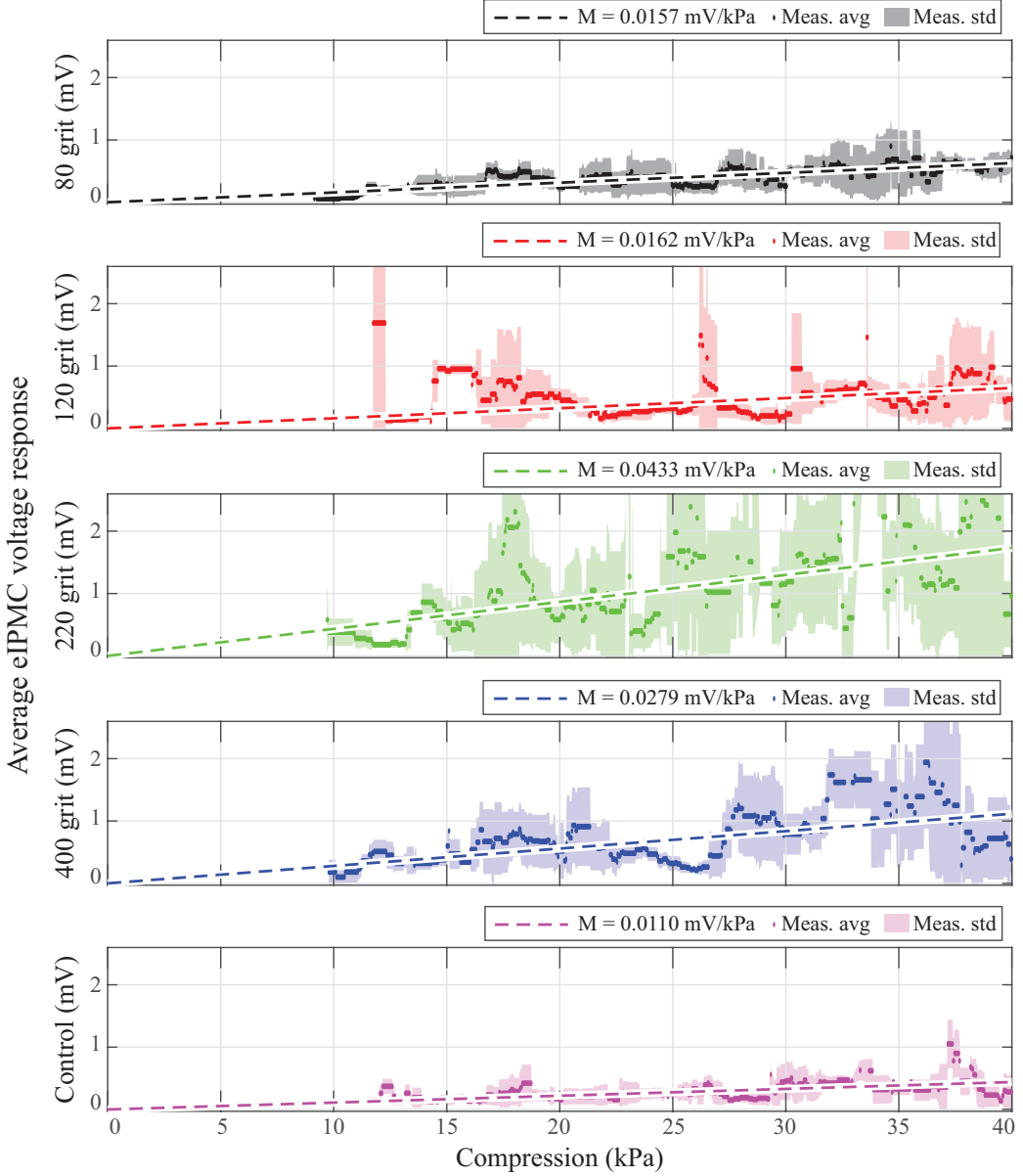


Figure 6. Compression pressure versus eIPMC sensor voltage responses with linear fit approximations.

The smoother surface 400 grit is second-most sensitive with 1.61 mV average response and 1.59 mV standard deviation, while the rougher-grit samples at 80 grit and 120 grit demonstrate less sensitivity (0.67 mV and 0.63 mV, respectively) and smaller variances (0.20 mV and 0.47 mV, respectively), although responses are still more sensitive than the control sensors. For this pressure magnitude, these results show that the polymer abrading technique effectively increases sensitivity over all surface roughnesses. However, these increases are not monotonic with grit size, and abrasions with the largest average size do not correspond to the most responsive sensors.

This peculiar behavior could be partially explained by observing that the engineered features on the polymer surface depend on the interplay of abrading feature size (*i.e.*, depth of grooves) and abrading feature density (*i.e.*, number of grooves per unit area). Obviously, small grits exhibit the largest features but also the smallest areal density, while the largest grit has smallest feature size but highest density. An intermediate grit size would

likely exhibit an optimum in the combination of the two competing factors and thus yield maximum sensitivity. Similarly, the more responsive sensors also demonstrate more variability in their open-circuit measurements between samples, likely due to the uncontrolled particle sizes in the sandpaper surface.

Lastly, the voltage response is averaged for all eIPMC sample swatches for a given grit rating over a range of applied pressures to observe the sensors' responsiveness beyond a single compression scenario. The average eIPMC voltage response is calculated between pressures of 0 and 40 kPa, where measurements within the range of  $\pm 1$  kPa are included for each average. Due to the experimental trials relying on loadings applied by hand, some pressures within this range are either unmeasured over all trials or consist of only a few observations. Linear regression is made for each sensor's experimental response normalized by the standard deviation, which is shown in Fig. 6. Again, the 220 grit sensors show the highest sensitivity with a fit of 0.0433 mV/kPa, an almost fourfold increase in sensitivity over the control sensor at 0.0110 mV/kPa. The next most sensitive eIPMC surface is fabricated with the 400 grit sandpaper (0.0279 mV/kPa), then the 120 grit surface (0.0162 mV/kPa) and 80 grit surface (0.0157 mV/kPa). Again, the more responsive eIPMC sensors also demonstrate more variance in the measured responses over all trials.

These experimental results demonstrate that the polymer abrading technique can be effectively used to fabricate eIPMCs through traditional manufacturing for standard IPMCs. Through the Nafion roughening procedure, surface particles around 53–74  $\mu\text{m}$  are the most successful in creating a sensitive compression sensor, although more controlled feature sizes will be necessary for future work to further identify the optimal surface roughness. Although more sensitivity has been demonstrated through this technique, the resulting variation in experiments shows that a more precise manufacturing method (*e.g.*, micromilling) may be preferable for the development of more repeatable eIPMC sensor behaviors or in determining optimal feature sizes in future eIPMC manufacturing approaches. Overall, the polymer abrading technique has been shown to be a viable method to enhance the sensitivity of IPMC compression sensors when additional manufacturing hardware for electrode feature construction is not available.

## 5. CONCLUSIONS

This work describes initial results of roughened engineered IPMC sensors for measuring forces and pressures under compression. A recently developed chemoelectromechanical model shows that asymmetry in the metal-polymer interface of eIPMCs increases the material's sensitivity in chemoelectromechanical transduction when under pressure. A polymer abrading technique is described to fabricate eIPMCs through traditional manufacturing methods and directed sanding procedures rather than through specialized material deposition hardware. Compression experiments on five sensor variants show consistently improved sensing performance for all the engineered samples versus the control, with up to a fourfold increase in sensitivity over the control sensor for a particular grit size of 220 using this fabrication method. Performance improves non-monotonically with grit size, which strongly points to the interplay of size and areal density of the abrasions on the polymer and their effect on the metal-polymer volume fraction at the engineered electrode. Future work will further improve the technique by identifying optimal particle sizes and densities for eIPMC fabrication to further improve sensitivity and better reduce its variability.

## Acknowledgments

This research was supported by the National Science Foundation under grants 1809455, 1809852, and 1545857. Any opinions, findings, and conclusions or recommendations expressed in this material are those of the authors and do not necessarily reflect the views of the sponsor.

## REFERENCES

- [1] Shahinpoor, M. and Kim, K. J., "Ionic polymer–metal composites: IV. Industrial and medical applications," *Smart Materials and Structures* **14**(1), 197 (2004).
- [2] Carrico, J. D., Traeden, N. W., Aureli, M., and Leang, K. K., "Fused filament 3D printing of ionic polymer–metal composites (IPMCs)," *Smart Materials and Structures* **24**(12), 125021 (2015).

- [3] Nakabo, Y., Mukai, T., and Asaka, K., “Biomimetic soft robots using IPMC,” in [*Electroactive Polymers for Robotic Applications*], 165–198, Springer (2007).
- [4] Aureli, M., Kopman, V., and Porfiri, M., “Free-locomotion of underwater vehicles actuated by ionic polymer metal composites,” *IEEE/ASME Transactions on Mechatronics* **15**(4), 603–614 (2009).
- [5] Carrico, J. D., Hermans, T., Kim, K. J., and Leang, K. K., “3D-printing and machine learning control of soft ionic polymer-metal composite actuators,” *Scientific Reports* **9**(1), 1–17 (2019).
- [6] Lei, H., Li, W., and Tan, X., “Microfabrication of IPMC cilia for bio-inspired flow sensing,” in [*Electroactive Polymer Actuators and Devices (EAPAD) 2012*], **8340**, 83401A, International Society for Optics and Photonics (2012).
- [7] McDaid, A., Xie, S., and Aw, K., “A compliant surgical robotic instrument with integrated IPMC sensing and actuation,” *International Journal of Smart and Nano Materials* **3**(3), 188–203 (2012).
- [8] Ming, Y., Yang, Y., Fu, R. P., Lu, C., Zhao, L., Hu, Y. M., Li, C., Wu, Y. X., Liu, H., and Chen, W., “IPMC sensor integrated smart glove for pulse diagnosis, Braille recognition, and human–computer interaction,” *Advanced Materials Technologies* **3**(12), 1800257 (2018).
- [9] Punning, A., Kruusmaa, M., and Aabloo, A., “Surface resistance experiments with IPMC sensors and actuators,” *Sensors and Actuators A: Physical* **133**(1), 200–209 (2007).
- [10] Lei, H., Sharif, M. A., and Tan, X., “Dynamics of omnidirectional IPMC sensor: Experimental characterization and physical modeling,” *IEEE/ASME Transactions on Mechatronics* **21**(2), 601–612 (2015).
- [11] MohdIsa, W., Hunt, A., and HosseinNia, S. H., “Sensing and self-sensing actuation methods for ionic polymer–metal composite (IPMC): A review,” *Sensors* **19**(18), 3967 (2019).
- [12] Ferrara, L., Shahinpoor, M., Kim, K. J., Schreyer, H. B., Keshavarzi, A., Benzel, E., and Lantz, J. W., “Use of ionic polymer–metal composites (IPMCs) as a pressure transducer in the human spine,” in [*Smart Structures and Materials 1999: Electroactive Polymer Actuators and Devices*], **3669**, 394–401, International Society for Optics and Photonics (1999).
- [13] Gudarzi, M., Smolinski, P., and Wang, Q.-M., “Compression and shear mode ionic polymer–metal composite (IPMC) pressure sensors,” *Sensors and Actuators A: Physical* **260**, 99–111 (2017).
- [14] Lee, J.-H., Chee, P.-S., Lim, E.-H., and Tan, C.-H., “Artificial intelligence-assisted throat sensor using ionic polymer–metal composite (IPMC) material,” *Polymers* **13**(18), 3041 (2021).
- [15] Volpini, V., Bardella, L., Rodella, A., Cha, Y., and Porfiri, M., “Modelling compression sensing in ionic polymer metal composites,” *Smart Materials and Structures* **26**(3), 035030 (2017).
- [16] Histed, R., Ngo, J., Hussain, O. A., Lapins, C. K., Fakharian, O., Leang, K. K., Liao, Y., and Aureli, M., “Ionic polymer metal composite compression sensors with 3D-structured interfaces,” *Smart Materials and Structures* **30**(12), 125027 (2021).
- [17] Aureli, M. and Porfiri, M., “Nonlinear sensing of ionic polymer metal composites,” *Continuum Mechanics and Thermodynamics* **25**(2), 273–310 (2013).
- [18] Orvis, K. H. and Grissino-Mayer, H. D., “Standardizing the reporting of abrasive papers used to surface tree-ring samples,” *Tree-Ring Research* **58**(1/2), 47–50 (2002).